Toward Organic Synthesis of a Magnetic Particle: Dendritic Polyradicals with 15 and 31 Centers for Unpaired Electrons

Andrzej Rajca* and Suchada Utamapanya

Contribution from the Department of Chemistry, University of Nebraska, Lincoln, Nebraska 68588-0304

*Received May 24, 1993**

Abstract: Starting from a bromo triether derivative **1**, we prepared a homologous pentadecaether, which is a precursor for the title pentadecaradical, by repeating twice the following two-step procedure (total of four steps): (1) Br/Li exchange followed by the addition of the organolithium to a benzoic acid ester derivative and (2) conversion of the triarylmethyl alcohol to methyl ether. Similarly, a 31-ether precursor was prepared by repeating three times the above sequence (total of six steps). The polyethers were converted with lithium metal in THF to the corresponding carbopolyanions and, subsequently, oxidized with iodine at 180 K to give the polyradicals. The polyradicals were studied in frozen THF and 2-MeTHF solutions by SQUID magnetometry in the 2–80 K temperature range and the 0–5.5-T magnetic field range; spin values, which are lower than expected for strong ferromagnetic coupling, were obtained. One of the possible explanations is the presence of defects, which disrupt ferromagnetic coupling between the triarylmethyl sites in these single-path π-conjugated systems; relationship of the current work to the percolation problem is discussed.

Introduction

Nanometer-size molecules have emerged as one of the exciting goals of organic synthesis related to materials science in the past few years.[1,2] The prospects for the emergence of solid-state properties in a single mesoscopic molecule are particularly enticing, but so far, adequate functionalization has not been achieved.

Very high-spin organic polyradicals approaching nanometer-size magnetic particles show the promise to address both fundamental aspects of quantum mechanics and important practical issues in magnetic materials; the examples are mesoscopic quantum tunneling and unusually strong anisotropies associated with nanometer-grained materials.[3,4] Organic polyradicals, especially hydrocarbons, should possess at least two distinct features compared to most metal-containing particles: (1) monodispersity and molecular shape control via organic synthesis and (2) negligible spin-orbit coupling.[5] These two features may allow for simple classical ab initio estimates of the magnetic anisotropy and facilitate observation of tunneling phenomena.

In the preliminary communication, we have reported the preparation and studies of the $S = {}^7/_2$ heptaradical and the $S = 5$ decaradical.[6] Now, we describe the synthesis of dendritic molecules with 15 and 31 centers (sites) for unpaired electrons and an attempt to prepare very high-spin polyradicals (Figure 1).

Connectivity between the triarylmethyl sites in the π-conjugated systems of polyradicals **4**[15·] and **5**[31·] is similar to the finite fragments of a 3-coordinated Cayley tree or Bethe lattice (Figure 2). Bethe lattices (and 1-dimensional linear chains) are one of the very few exactly solvable problems in percolation phenomena, related to phase transitions and, in particular, magnetism.[7] Dendritic macromolecules should be superior over conventional linear macromolecules in regard to spin ordering in a single molecule.[7,8]

Results and Discussion

Synthesis. Primary synthetic targets, dendritic polyethers **4-OMe-(OMe)$_{14}$** and **5-OMe-(OMe)$_{30}$** (Figure 1), are constructed by a convergent route starting from bromo ether **1** (Figure 3).[9]

The Br/Li exchange (step A) is followed by double addition of aryllithium to methyl 3-bromo-2,4-dimethylbenzoate (step B). The resultant triarylmethyl alcohol **2-OH-(OMe)$_6$-Br** is isolated

* Abstract published in *Advance ACS Abstracts*, October 15, 1993.

(1) Tomalia, D. A.; Naylor, A. M.; Goddard, W. A., III. *Angew. Chem., Int. Ed. Engl.* **1990**, *29*, 138. Mekelburger, H.-B.; Jaworek, W.; Vogtle, F. *Angew. Chem., Int. Ed. Engl.* **1992**, *31*, 1571.

(2) (a) Miller, L. L.; Kenny, P. W. *J. Chem. Soc., Chem. Commun.* **1988**, 84. (b) Tomalia, D. A.; Baker, H.; Dewald, J.; Hall, M.; Kallos, G.; Martin, S.; Roeck, J.; Ryder, J.; Smith, P. *Polym. J.* **1985**, *17*, 117. Tomalia, D. A.; Baker, H.; Dewald, J.; Hall, M.; Kallos, G.; Martin, S.; Roeck, J.; Ryder, J.; Smith, P. *Macromolecules* **1986**, *19*, 2466. (c) Newkome, G. R.; Yao, Z.; Baker, G. R.; Gupta, V. K. *J. Org. Chem.* **1985**, *50*, 2004. Newkome, G. R.; Baker, G. R.; Saunders, M. J.; Russo, P. S.; Gupta, V. K.; Yao, Z.; Bouillion, J. E. *J. Chem. Soc., Chem. Commun.* **1986**, 752. Newkome, G. R.; Moorefield, C. N.; Baker, G. R.; Saunders, M. J.; Grossman, S. H. *Angew. Chem., Int. Ed. Engl.* **1991**, *30*, 1178. Newkome, G. R.; Arai, S.; Fronczek, F. R.; Moorefield, C. N.; Lin, X.; Weis, C. D. *J. Org. Chem.* **1993**, *58*, 898. (d) Wooley, K. L.; Hawker, C. J.; Fréchet, J. M. J. *J. Am. Chem. Soc.* **1991**, *113*, 4252. Hawker, C. J.; Fréchet, J. M. J. *J. Am. Chem. Soc.* **1990**, *112*, 7638. Hawker, C. J.; Fréchet, J. M. J. *Macromolecules* **1990**, *23*, 4726. (e) Kwock, E. W.; Neenan, T. X.; Miller, T. M. *Chem. Mater.* **1991**, *3*, 775. Miller, T. M.; Neenan, T. X. *Chem. Mater.* **1990**, *2*, 347. Miller, T. M.; Neenan, T. X.; Zayas, R.; Bair, H. E. *J. Am. Chem. Soc.* **1992**, *114*, 1018. Miller, T. M.; Neenan, T. X.; Kwock, E. W.; Stein, S. M.; *J. Am. Chem. Soc.* **1993**, *115*, 356. (f) Moore, J. S.; Xu, Z. *Macromolecules* **1991**, *24*, 5893. Moore, J. S.; Zhang, J. *Angew. Chem., Int. Ed. Engl.* **1992**, 31, 922. (g) Uchida, H.; Kabe, Y.; Yoshino, K.; Kawamata, A.; Tsumuraya, T.; Masamune, S. *J. Am. Chem. Soc.* **1990**, 112, 7077. (h) Rengan, K.; Engel, R. *J. Chem. Soc., Chem. Commun.* **1990**, 1084. (i) Rajca, A. *J. Org. Chem.* **1991**, 56, 2557.

(3) For reviews on high-spin molecules, see: Iwamura, H. *Adv. Phys. Org. Chem.* **1990**, *26*, 179. Dougherty, D. A. *Acc. Chem. Res.* **1991**, *24*, 88.

(4) For small magnetic particles and nanostructured solids, see: (a) Awschalom, D. D.; DiVincenzo, D. P.; Smyth, J. F. *Science* **1992**, *258*, 414. (b) Bucher, J. P.; Douglass, D. C.; Bloomfield, L. A. *Phys. Rev. Lett.* **1991**, *66*, 3052. de Heer, W. A.; Milani, P.; Chatelain, A. *Phys. Rev. Lett.* **1990**, *65*, 488. (c) Chien, C. L. In *Recent Advances in Magnetism and Magnetic Materials*; Huang, H. L., Kuo, P. C., Eds.; World Scientific: Singapore, London, 1989; pp 296–319.

(5) Rajca, A.; Utamapanya, S. *Liq. Cryst. Mol. Cryst.* **1993**, *232*, 305.

(6) Rajca, A.; Utamapanya, S.; Thayumanavan, S. *J. Am. Chem. Soc.* **1992**, *114*, 1884.

(7) Stauffer, D. *Introduction to Percolation Theory*; Taylor and Francis: London, 1985. Stauffer, D. *Phys. Rep.* **1979**, *54*, 1. Guemez, J.; Velasco, S. *Physica A* **1991**, *171*, 486.

(8) (a) For example, defects are less likely to interrupt nearest neighbor coupling in a Bethe lattice compared to that in a 1-dimensional linear chain. In dendritic molecules (fragments of Bethe lattices), about half of the available sites are oblivious to defects because they are at the periphery of the molecule (fragment of lattice); also, some defects at the inner sites may be tolerated. In the language of percolation, a nearest neighbor connection from one end to the other end of the dendritic molecule may be found as long as the overall nondefect density p is larger than the critical value p_c percolation threshold. For a 3-coordinated Bethe lattice, $p_c = {}^1/_2$, and for a 1-dimensional linear chain, $p_c = 1$; practically, there is no allowance for defects in linear chain macromolecules. (b) For a defective high-spin linear chain polymer, see: Utamapanya, S.; Kakegawa, H.; Bryant, L.; Rajca, A. *Chem. Mater.* **1993**, *5*, 1053.

(9) Reference 2i and Rajca, A.; Janicki, S., in preparation.

0002-7863/93/1515-10688$04.00/0

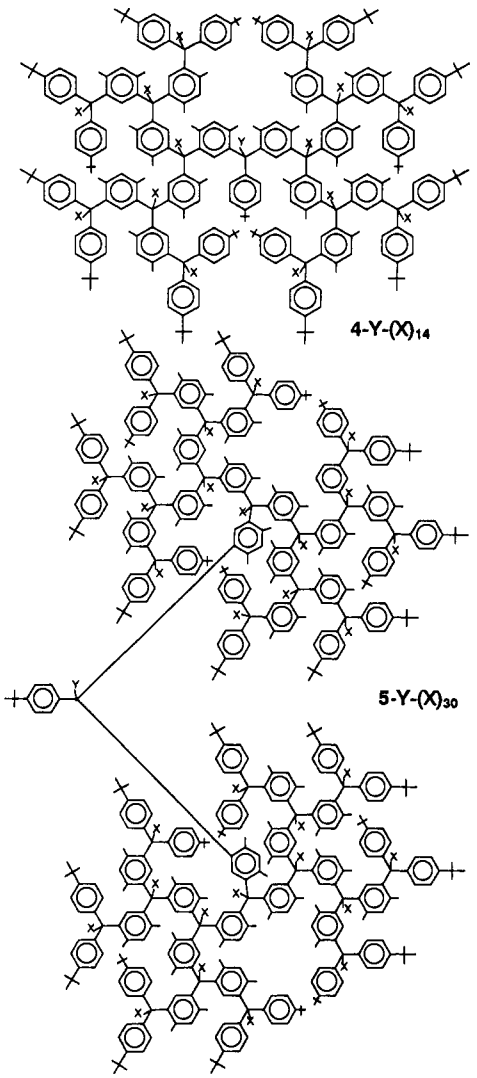

Figure 1. Target molecules. Dendritic polyarylmethanes and polyarylmethyls with Y = OH and X = OMe (**4-OH-(OMe)$_{14}$** or **5-OH-(OMe)$_{30}$**), Y = X = OMe (**4-OMe-(OMe)$_{14}$** or **5-OMe-(OMe)$_{30}$**), Y = X = –, Li^+, Y = X = unpaired electron ($4^{15\cdot}$ or $5^{31\cdot}$), and Y = X = H (**4-H-(H)$_{14}$** or **5-H-(H)$_{30}$**).

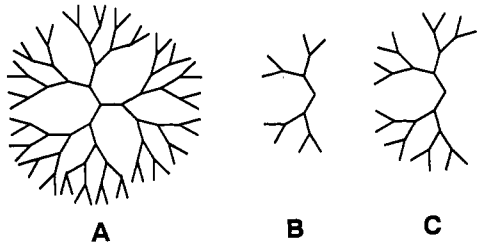

Figure 2. *A*: fragment of a 3-coordinated Cayley tree (Bethe lattice). B and *C*: connectivities between triarylmethyl sites in the dendritic π-conjugated polyradicals $4^{15\cdot}$ and $5^{31\cdot}$.

and, then, converted to the corresponding methyl ether **2-OMe-(OMe)$_6$-Br** (step D). Further homologation of **2-OMe-(OMe)$_6$-Br** using the above sequence (steps AB and D) gives **3-OMe-(OMe)$_{14}$-Br**. After the last two compounds are converted to the corresponding aryllithiums (step A), the double additions to methyl 4-*tert*-butylbenzoate give the intermediate triarylmethyl alcohols (step C), which are isolated and converted to the corresponding methyl ethers **4-OMe-(OMe)$_{14}$** and **5-OMe-(OMe)$_{30}$** (step D).

The isolated products consist of an alcohol/ether sequence: $R_1OH \rightarrow R_1OMe \rightarrow R_2OH \rightarrow R_2OMe \rightarrow \ldots \rightarrow R_nOH \rightarrow R_n$-OMe; the molecular weight between the consecutive alcohols is

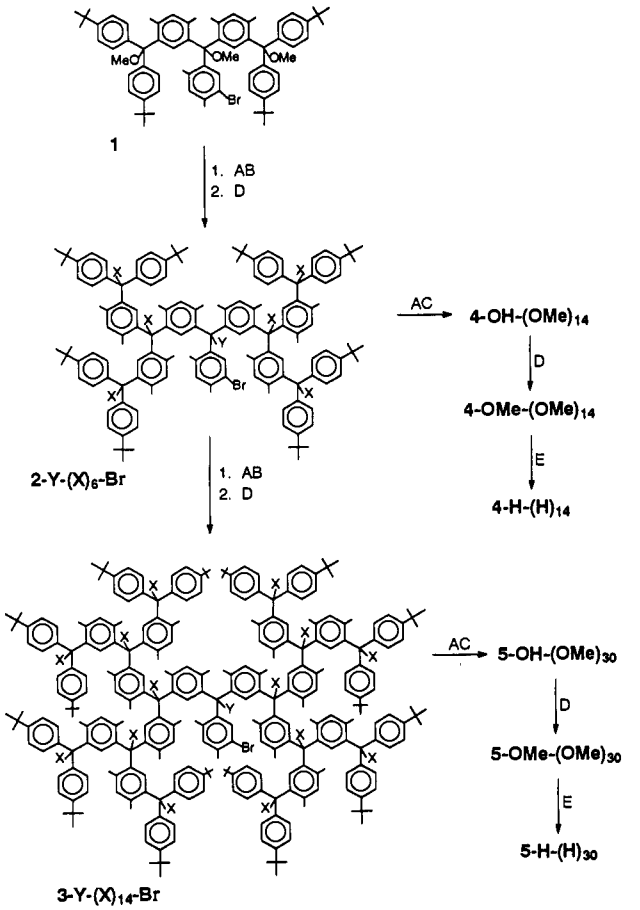

Figure 3. Synthesis of the polyether precursors for the polyradicals and their derivatives: (A) *t*-BuLi, ether; (B) methyl 3-bromo-2,4-dimethylbenzoate; (C) methyl 4-*tert*-butylbenzoate; (D) NaH/DMF, MeI; and (*E*) Li/THF, MeOH.

approximately doubled, and all compounds, including those with the highest molecular weights, are well soluble in aprotic solvents. The alternating polarity in each step and the increase of molecular weight in every other step (ether → alcohol) are favorable for chromatographic separation by a standard silica column. Thus, in the ether → alcohol conversion, the alcohol product shows a TLC spot significantly below that of the reactant ether; in the alcohol → ether case, the product is slightly above the reactant, except for the highest molecular weight pair **5-OH-(OMe)$_{30}$** → **5-OMe-(OMe)$_{30}$**, where the spots are indistinguishable by short-path TLC. Yields for all isolated products are 50% or higher, except for step AC involving the transformation of **3-OMe-(OMe)$_{14}$-Br** to **5-OH-(OMe)$_{30}$**, which is only 40%.

Characterization of such large and sterically congested molecules poses a challenge. Because of the polymeric nature of these dendritic molecules, C/H analyses are similar for all compounds and, therefore, they are of little value in structure determination as observed for analogous star-branched molecules.[2i] All alcohols, except for **5-OH-(OMe)$_{30}$** which is not available in a sufficient amount, and polyethers give acceptable C/H analyses.

NMR spectra are typically broad and useful as a "fingerprint" because a plethora of isomers, which interconvert on different time scales, is associated with sterically hindered triarylmethyl centers.[9,10,17] In an attempt to decrease the steric congestion, the OMe groups are replaced with hydrogens by reduction of the

(10) For propeller isomerism, see: Mislow, K. *Acc. Chem. Res.* **1976**, *9*, 26.

(11) (a) Rajca, A.; Utamapanya, S. *J. Am. Chem. Soc.* **1993**, *115*, 2396. (b) Rajca, A.; Utamapanya, S. *J. Org. Chem.* **1992**, *57*, 1760. (c) Rajca, A.; Utamapanya, S.; Xu, J. *J. Am. Chem. Soc.* **1991**, *113*, 9235. (d) Utamapanya, S.; Rajca, A. *J. Am. Chem. Soc.* **1991**, *113*, 9242. (e) Rajca, A. *J. Am. Chem. Soc.* **1990**, *112*, 5889, 5890.

Table I. Summary of FAB Mass Spectroscopy Data[a]

compound	M^+ at m/e	$(M - OCH_3)^+$ at m/e
2-OH-(OMe)$_6$-Br, found		2129, 2130, 2131, 2132
M = $C_{149}H_{179}O_7Br$, calcd		2129, 2130, 2131, 2132
2-OMe-(OMe)$_6$-Br, found		2143, 2144, 2145, 2146
M = $C_{150}H_{181}O_7Br$, calcd		2143, 2144, 2145, 2146
2-H-(H)$_6$-Br, found	1963, 1964, 1965, 1966	
M = $C_{143}H_{167}Br$, calcd	1964, 1965, 1966, 1967	
3-OH-(OMe)$_{14}$-Br, found		4372, 4373, 4374*, 4375
M = $C_{309}H_{371}O_{15}Br$, calcd		4373, 4374*, 4375, 4376
3-OMe-(OMe)$_{14}$-Br, found		4385, 4386, 4387, 4388*
M = $C_{310}H_{373}O_{15}Br$, calcd		
4-OH-(OMe)$_{14}$, found		4322, 4323, 4324
M = $C_{311}H_{376}O_{15}$, calcd		4322, 4323, 4324
4-OMe-(OMe)$_{14}$, found		4336, 4337, 4338
M = $C_{312}H_{378}O_{15}$, calcd		4336, 4337, 4338
4-O[^{13}C]Me-(OMe)$_{14}$, found		4337, 4338, 4339
M = $C_{311}[^{13}C_1]H_{376}O_{15}$, calcd		
4-H-(H)$_{14}$, found	3916, 3917, 3918*	
M = $C_{297}H_{348}$, calcd	3917, 3918*, 3919	
5-OH-(OMe)$_{30}$, found		8810
M = $C_{631}H_{760}O_{31}$, calcd		8810
5-OMe-(OMe)$_{30}$, found		8823
M = $C_{632}H_{762}O_{31}$, calcd		8824

[a] The most intense peaks are shown for the M^+ or $(M - OCH_3)^+$ clusters; an asterisk indicates the highest peak. For the ions with $m/e > 8000$ Da, only average mass peaks are observed.

ethers with lithium metal in THF followed by protonation of the resultant carbanion (step E in Figure 3); in the case of **2-OMe-(OMe)$_6$-Br**, reduction to **2-H-(H)$_6$-Br** is accomplished using sodium borohydride in CF_3COOH/MeOH.[9] The ^{1}H NMR spectrum for **2-H-(H)$_6$-Br** at 370 K allows for partial resolution of the resonances associated with the triarylmethane protons. For all other compounds, the ^{1}H NMR spectra are unresolved. Also, the "middle" OMe group, which is 99% ^{13}C in **4-O[^{13}C]-Me-(OMe)$_{14}$**, appears as a broad resonance at 52.5 ppm in the standard proton-decoupled and ^{13}C DEPT NMR spectra between 295 and 350 K.[17]

IR spectra indicate the presence of the OH group in each alcohol (3200–3700 cm^{-1}) and its absence in the corresponding polyethers.[17]

FAB mass spectra show the expected ions (Table I). For all Br-containing compounds, the expected distortion of the isotopic intensities is found. For **4-OMe-(OMe)$_{14}$**, it is found that the isotopic intensities for the $(M - OCH_3)^+$ ion from **4-OMe-(OMe)$_{14}$** are in satisfactory agreement with the calculated ones and, upon ^{13}C-labeling, the $(M - OCH_3)^+$ isotopic multiplet for **4-O[^{13}C]-Me-(OMe)$_{14}$** is shifted by $m/e = 1$ Da. Also, the expected $m/e = 14$ Da shift (by CH_2) between **4-OH-(OMe)$_{14}$** and **4-OMe-(OMe)$_{14}$** is obtained. For the higher homologues **5-OH-(OMe)$_{30}$** and **5-OMe-(OMe)$_{30}$**, which are in the mass range of 8000+ Da, isotopic peaks can not be resolved; because ±1-Da mass calibration in this high m/e range is difficult, the agreement between the observed shift of $m/e = 13$ Da and the theoretical shift of $m/e = 14$ Da is satisfactory.[17]

Two polyether precursors are converted to polyradicals with 15 and 31 sites for unpaired electrons (eq 1). The final product

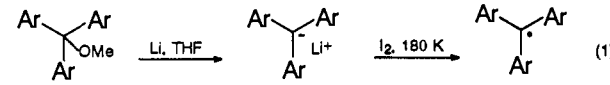

4-OMe-(OMe)$_{14}$ **4$^{15\cdot}$**

5-OMe-(OMe)$_{30}$ **5$^{31\cdot}$**

in eq 1 is a sample of the polyradical in THF or 2-MeTHF for SQUID measurements. Chemistry and technical procedures for sample preparation follow those developed for the lower homologues as described elsewhere.[6,11]

Magnetic Measurements and Their Interpretation. The two types of SQUID measurements carried out are (1) magnetization (M) vs magnetic field (H) at low temperatures (T) and (2) M vs T at low H. The data are plotted as M vs H/T (at $T = 2$, 5, and 10 K) and MT vs T (at $H = 0.5$ or 1.0 T), respectively. The MT vs T plots show downward curvature at $T < 20$ K, and the M vs H/T plots show the temperature-dependent curvature; these features are consistent with the presence of antiferromagnetic (AFM) interactions. A simple mean-field replacement of T with $T - \theta$ accounts for the AFM interactions ($\theta < 0$),[12] e.g., for **4$^{15\cdot}$** and **5$^{31\cdot}$** in THF or 2-MeTHF, $0 > \theta > -0.7$ K. For the strongly coupled high-spin polyradicals **4$^{15\cdot}$** and **5$^{31\cdot}$**, a single Brillouin function corresponding to $S = {}^{15}/_2$ and ${}^{31}/_2$, respectively, should describe the magnetization data after correction for intermolecular magnetic interactions.[11a] However, the above M vs $H/(T - \theta)$ data can not be satisfactorily fit to a single Brillouin function. For **4$^{15\cdot}$**, at low and high H/T, the $S \approx {}^7/_2$ and the $S \approx {}^5/_2$ Brillouin functions are followed, respectively; for **5$^{31\cdot}$**, the Brillouin functions correspond to even lower spin, $S \approx {}^5/_2$ and $S \approx {}^4/_2$.

(12) (a) Carlin, R. L. *Magnetochemistry*; Springer-Verlag: New York, 1986. (b) Bino, A.; Johnston, D. C.; Goshorn, D. P.; Halbert, T. R.; Stiefel, E. I. *Science* **1988**, *241*, 1479.

(13) Magnetization M is related via a spin-independent factor to the product SB_S, where Brillouin function B_S corresponds to spin S; thus, at small H/T, $M \propto S(S+1)$, and at the other limit of large H/T, $M \propto S$ (ref 12a). Therefore, the addition of magnetizations, const$_1 S_1 B_{S1}$ and const$_2 S_2 B_{S2}$ for *different* spins, $S_1 \neq S_2$, does not result in a product of spin and Brillouin function, SB_S. In particular, the molar magnetization for an equimolar mixture of two spin systems, $S_1 \neq S_2$, follows the Brillouin functions corresponding to $S' = [(1 + 2A)^{1/2} - 1]/2$, where $A = S_1(S_1 + 1) + S_2(S_2 + 1)$, at small H/T and $S'' = (S_1 + S_2)/2$ at large H/T, i.e., there is a crossover from the larger S' to the smaller S'' function with increasing H/T. Analogous results are easily obtained for more than two spin systems.

(14) The present value of μ_{eff} in the SQUID samples of **10$^{10\cdot}$** in THF can be compared to $\mu_{eff} = 11\ \mu_B$ for **10$^{10\cdot}$** in Me_2O, which was measured using NMR spectroscopy (ref 6).

(15) Probability P includes some spin systems with a relatively small S.

(16) The magnetic anisotropy barrier E_A for the inversion of the magnetization vector (superparamagnetic relaxation) is estimated in the homologues of **4$^{15\cdot}$** and **5$^{31\cdot}$** using dipolar contributions only and assuming ellipsoidal shape. $E_A = ({}^1/_2)NI_s^2V$ is a product of the demagnetizing factor ($N = 0$ for a sphere and $N = 2\pi$ for an infinitely elongated needle), square of magnetization, and volume associated with the spin systems. For one unpaired electron per 250 Da and density of 1 g/cm^3, there is 2.4×10^{21} electrons/cm^3. Because the magnetic moment of an electron is 0.93×10^{-20} erg/Gs, $I_s = (2.4 \times 10^{21})$ $(0.93 \times 10^{-20}) \approx 22$ in CGS units. Having n_{el} unpaired electrons and volume per electron $1/(2.4 \times 10^{21})$, $V = n_{el}(0.42 \times 10^{-21})$ cm^3. For a moderately elongated shape, $N = 3$ is assumed. With the above assumptions, $E_A \approx 3n_{el} \times 10^{-19}$ erg; thus, for $n_{el} > 100$, $E_A > 3 \times 10^{-17}$ erg. For observation of an imaginary component in AC susceptibility due to slow (on the experimental time scale) superparamagnetic relaxation, typically, E_A must be significantly greater than kT; thus, $n_{el} > 100$ and $T < 0.1$ K or $n_{el} > 1000$ and $T < 1$ K. For references, see: Craik, D. J.; Tebble, R. S. *Ferromagnetism and Ferromagnetic Domains*; North-Holland and Wiley: New York, 1965.

(17) See the supplementary material.

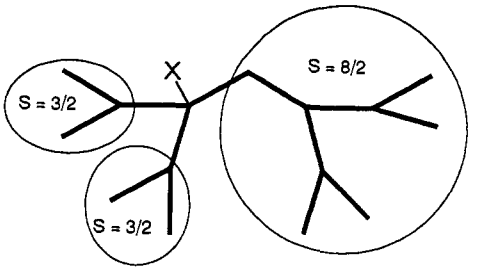

Figure 4. Connectivity in the pentadecaradical $4^{15\cdot}$ with one defect (X) at one of the inner triarylmethyl sites.

Definite interpretation of these magnetic data is difficult. Initially, one of the possible explanations, which is based upon defects, is given, and a simplistic quantitative model is fitted to the data for $4^{15\cdot}$ and $5^{31\cdot}$. Then, this model is applied to the magnetic data for the previously studied high-spin di-, tetra-, hepta-, and decaradicals, which are the lower homologues of $4^{15\cdot}$ and $5^{31\cdot}$. Finally, one of possible alternative explanations for magnetic data in $4^{15\cdot}$ and $5^{31\cdot}$ is discussed.

The Brillouin function crossing may be accounted for when each polyradical does not consist of a single $S = {}^{15}/_{2}$ or $S = {}^{31}/_{2}$ spin system but two or more noninteracting spin systems with different values of S.[13] These interruptions of spin coupling in the polyradicals may arise when defects are present in the π-conjugated system, e.g., a 4-coordinated sp^3-hybridized carbon in the place of a sp^2-hybridized carbon with an unpaired electron at the triarylmethyl site. Because generation of polyradicals involves sequential reactions (eq 1) at 15 or 31 sites, defects, which are failures to generate an unpaired electron, are likely, even if the yields per site for each reaction are good. Such a defect may arise when the intermediate carbopolyanion (eq 1) is protonated, the polyradical is iodinated at one of the triarylmethyl sites, or CC bonds are formed between the sterically congested branches of the molecules, etc. Defects at the inner triarylmethyl sites are quite detrimental to spin coupling, and even a modest number of them has a dramatic impact on the magnetic data. As shown in Figure 4, one defect in $4^{15\cdot}$ may give a polyradical, which consists of three spin systems, $S = {}^{8}/_{2}$, ${}^{3}/_{2}$, and ${}^{3}/_{2}$; for this particular monodefected polyradical, the magnetization should "cross" from the $S \approx 2.6$ to the $S \approx 2.3$ Brillouin functions at low and high H/T, respectively.[13]

In order to numerically fit the magnetic data, it is assumed, similarly to many percolation problems,[7] that the defects are distributed with equal probability, that is, the probability for having an unpaired electron ("no defect") is p for each triarylmethyl site. For $4^{15\cdot}$, about 7000 spin systems for polyradicals with zero to four defects are enumerated. The larger number of defects are handled approximately, i.e., for five and six defects, the $S = {}^{5}/_{4}$ and $S = {}^{15}/_{14}$ Brillouin functions are used. This approximation tends to overestimate p. All Brillouin functions are added numerically with the appropriate weighing factors to fit the experimental magnetization by simultaneous variation of p and the number of moles of polyradical n in the sample. The fit gives $p = 0.80$, that is, with the above equal probability assumption, the yield for the generation of unpaired electrons in $4^{15\cdot}$ from pentadecaether **4-OMe-(OMe)$_{14}$** is only 80% per site (eq 1; Figure 5). For $5^{31\cdot}$, polyradicals with 0–13 defects are treated approximately giving an upper bound for p, which is 0.78.

The above procedure for analyzing magnetization data, using the exact enumeration of spin systems for polyradicals with zero to four defects, is applied to the lower homologues of $4^{15\cdot}$ and $5^{31\cdot}$, i.e., diradical $6^{2\cdot}$, tetraradical $7^{4\cdot}$, heptaradical $8^{7\cdot}$, heptaradical $9^{7\cdot}$, and decaradical $10^{10\cdot}$ (Figure 6).[5,6,11ac]

Fitting to magnetization vs $H/(T-\theta)$ gives p values from 0.93 to 0.96; these values are higher than $p = 0.8$ for the larger homologues (Figure 6). For $6^{2\cdot}$, for which $p = 0.96$, the experimental magnetization is indistinguishable from the $S = 1$ Brillouin function (Figure 7). For polyradicals with a larger number of triarylmethyl centers, the discrepancies between the theoretical Brillouin functions for "perfect" high-spin polyradicals and the actual magnetization become more pronounced. For $9^{7\cdot}$

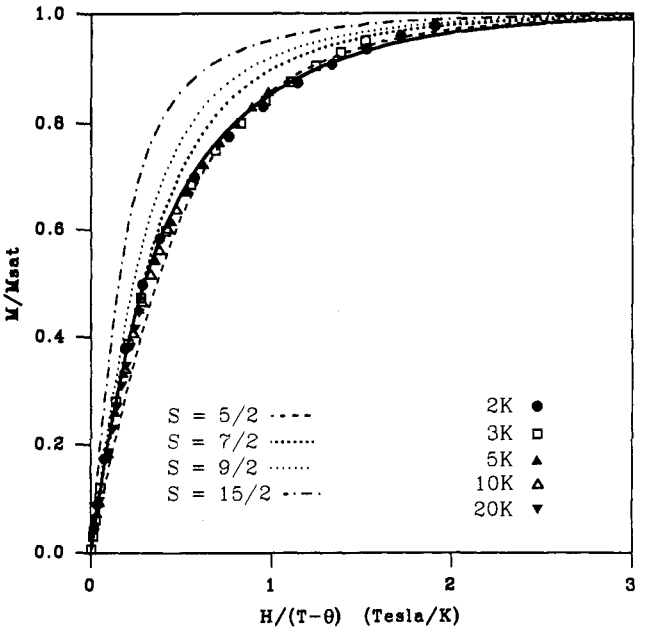

Figure 5. Magnetization data for the dendritic pentaradical $4^{15\cdot}$ in 2-MeTHF; $\theta = -0.63$ K. Solid and intercepted lines correpond to a fit with $p = 0.80$ and Brillouin function plots, respectively.

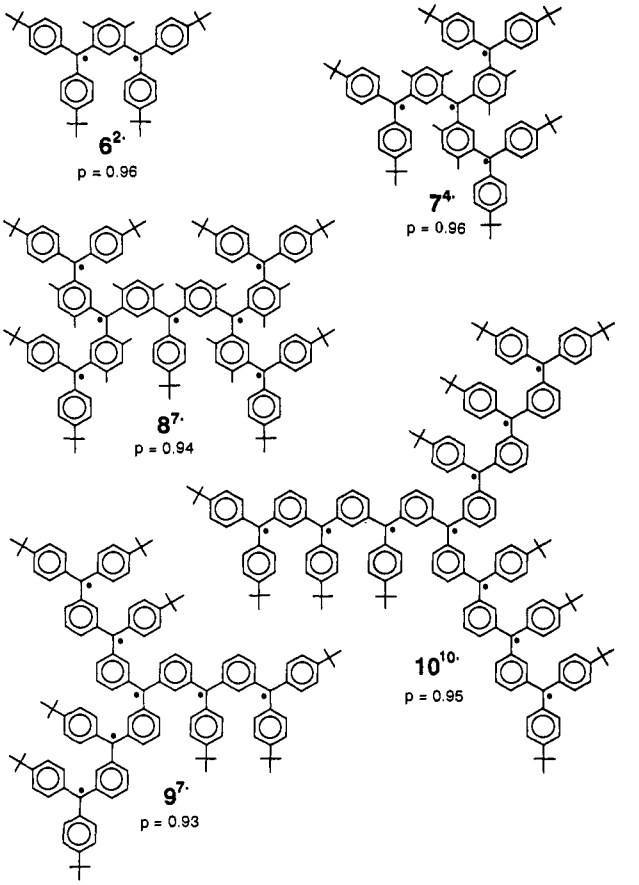

Figure 6. Structures for the previously prepared di-, tetra-, hepta-, and decaradicals $6^{2\cdot}$, $7^{4\cdot}$, $8^{7\cdot}$, $9^{7\cdot}$, and $10^{10\cdot}$. The magnetization data are fit, assuming equal probability p for having an unpaired electron at any given triarylmethyl site. The following numbers of defects are considered and treated exactly: diradical, 0–1, tetraradical, 0–3, and hepta- and decaradicals, 0–4 (Figures 7 and 8).

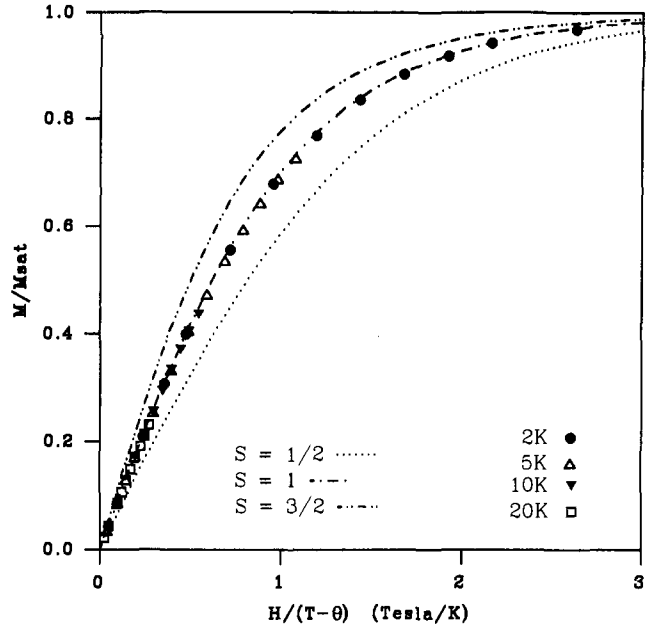

Figure 7. Magnetization data for diradical $6^{2\cdot}$ in 2-MeTHF; $\theta = -0.09$ K. The fit with $p = 0.96$ is not shown. Intercepted lines are Brillouin function plots.

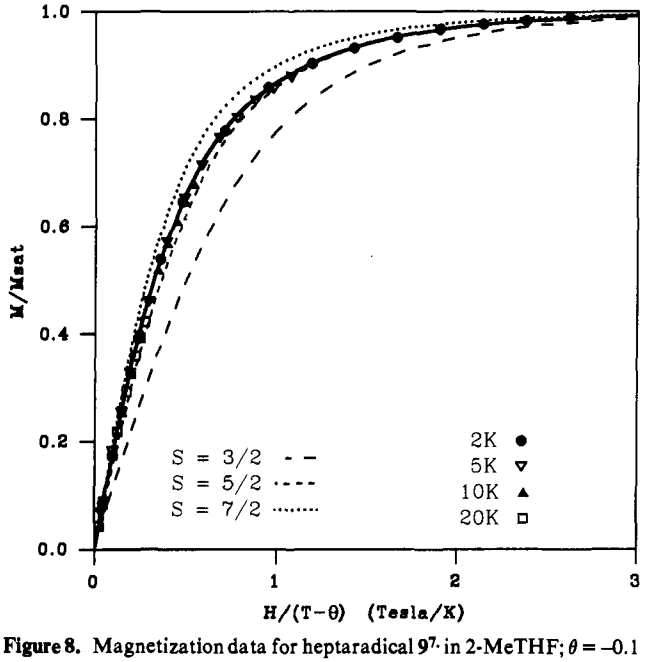

Figure 8. Magnetization data for heptaradical $9^{7\cdot}$ in 2-MeTHF; $\theta = -0.1$ K. Solid and intercepted lines correspond to a fit with $p = 0.93$ and Brillouin function plots, respectively.

with $p = 0.93$, the magnetization switches from the $S \approx {}^6/_2$ to the $S \approx {}^5/_2$ Brillouin function with increasing $H/(T-\theta)$ rather than following the $S = {}^7/_2$ Brillouin function as expected for the $S = {}^7/_2$ heptaradical (Figure 8). The effective magnetic moments μ_{eff} are calculated using the number of moles of polyradical from the fit and the MT vs T data. μ_{eff} are comparable to the theoretical values for the defect-free polyradicals, e.g., 9.9 μ_B for $\mathbf{10}^{10\cdot}$ in THF vs the theoretical value of 11.0 μ_B.[14]

Why does p decrease drastically for polyradicals with 15 and 31 centers compared to polyradicals with 2–10 centers? This apparent decrease in p suggests problems with the chemistry of the generation or persistence of $\mathbf{4}^{15\cdot}$ and $\mathbf{5}^{31\cdot}$. For large, sterically congested $\mathbf{4}^{15\cdot}$ and $\mathbf{5}^{31\cdot}$, the reactions in eq 1 at their inner centers may not be efficient.

The previous spectroscopic studies of carbopolyanions, which are analogous to those in eq 1, suggest increasing negative charge density from the outer to the inner triarylmethyl sites,[11de] that is, for the carbopolyanions in eq 1, the inner triarylmethyl sites may be more readily protonated by the solvent or impurities. Also, it was shown that radical anions (or polyradical polyanions) are intermediates in the generation of carbopolyanions from polyethers;[11d] in the sterically congested environment at the inner centers of the compounds in eq 1, two polyradical polyanion "branches" of the dendrimer may intramolecularly "dimerize" to create two defects. If the inner centers in $\mathbf{4}^{15\cdot}$ and $\mathbf{5}^{31\cdot}$ are especially defect-prone, that is, the "equal probability" assumption for the defects does not apply to $\mathbf{4}^{15\cdot}$ and $\mathbf{5}^{31\cdot}$, the magnetization is profoundly affected as illustrated in Figure 4 and the preceding discussion. Consequently, with the uneven distribution of defects, the overall yield per site may still be close to 90% for $\mathbf{4}^{15\cdot}$ and $\mathbf{5}^{31\cdot}$ but their "average" spin values are comparable to the polyradicals with only 7 or 10 sites for unpaired electrons. The unequal probability in distribution of defects (and approximations for five and six defects) may be the cause of discrepancies between the fit and the magnetization data for $\mathbf{4}^{15\cdot}$ (Figure 5).

The yield per unpaired electron, $p \approx 0.8$, for dendritic polyradicals $\mathbf{4}^{15\cdot}$ and $\mathbf{5}^{31\cdot}$ is still significantly above the percolation threshold, $p_c = 0.5$, for a 3-coordinated Bethe lattice.[7] If $p > p_c$ and the p's are identical at all sites, the probability P for having a spin system extending throughout the molecule (lattice) is $P > 0$;[15] in particular, $P = p\{1 - [(1-p)/p]^3\}$, which gives $P \approx 0.8$ for $p \approx 0.8$.[7]

A large overall defect rate and a significant number of defects at the inner triarylmethyl sites are only some of the possible interpretations for the interruption of the ferromagnetic coupling in $\mathbf{4}^{15\cdot}$ and $\mathbf{5}^{31\cdot}$. It has been reported that ferromagnetic coupling remains strong upon extension of conjugation, e.g., $\mathbf{10}^{10\cdot}$, or steric congestion, e.g., $\mathbf{7}^{4\cdot}$, with *i*-Pr groups replacing the Me groups.[6,11a] It is plausible that in $\mathbf{4}^{15\cdot}$ and $\mathbf{5}^{31\cdot}$, which are both extended and sterically hindered, the spin coupling is weakened to the extent that some parts of the polyradical become effectively uncoupled on the energy scale of the measurement, e.g., intramolecular AFM coupling between the dendrimer branches may offset through-bond ferromagnetic interactions. The present magnetic measurements do not allow to establish rigorously the cause for the interruption of the ferromagnetic coupling in $\mathbf{4}^{15\cdot}$ and $\mathbf{5}^{31\cdot}$.

Conclusion

For 1,3-connected polyarylmethyl polyradicals with 15 and 31 sites for unpaired electrons, the average spin is comparable to those for the homologues with 7 or 10 sites.[6] This apparent low average is most likely associated with defects in these π-conjugated systems, but other reasons may not be excluded at this time.

In the current static magnetization measurements, a plethora of low-spin systems, $S = {}^1/_2$ and $S = {}^2/_2$, etc., effectively disguises very high-spin systems, which might be present in $\mathbf{4}^{15\cdot}$ and $\mathbf{5}^{31\cdot}$. Very high-spin systems in the presence of a large number of low-spin systems may be detected by AC magnetometry at low temperature, that is, the magnetic anisotropy associated with the very high spins preformed into elongated shapes of the dendritic molecules should lead to a nonzero imaginary part of the magnetic susceptibility. Our estimate is that 1,3-connected polyarylmethyls with >100 unpaired electrons may allow such measurement at very low temperature.[16] Synthesis of at least the next two higher homologues of $\mathbf{5}^{31\cdot}$ is required.

Improving chemical yield and designing strongly coupled, multiple closed-loop systems are alternative approaches to defeat the defects.

Experimental Section

The glovebox and vacuum line were already described.[11a] Ether and tetrahydrofuran (THF) for use on the vacuum line were distilled from purple sodium/benzophenone in a nitrogen atmosphere immediately before

use. Hamilton gas-tight syringes were used for all liquid transfers. Methyl 5-bromo-2,4-dimethylbenzoate, methyl 4-*tert*-butylbenzoate, and bromo ether **1** were previously prepared in this laboratory.[9] All other chemicals were obtained from Aldrich; in particular, "high in sodium" (98+%) lithium metal was used.

For thin-layer chromatography (TLC), Analtech silica glass plates with hexane/ether as eluent were used. For column chromatography, Davisil silica (pH = 6.5, 200–425 mesh, 60 Å) with hexane/ether as eluent was used; the elution pressure was 20 psig.

NMR spectra were obtained using Omega spectrometers (^{1}H NMR at 500 and 300 MHz) in the 295–370 K temperature range. Solvents were C_6D_6 or tetrachloroethane/C_6D_6 (10/1); the last solvent mixture is designated as TCE/C_6D_6. The spectra possess three characteristic regions: aromatic (8–5.5 ppm), Me and OMe groups (3.3–1.4 ppm), and *tert*-Bu groups (1.4–0.9 ppm). Integrations are unreliable because of the spectral broadness and the large number of protons involved; this is especially the case for the large homologues. Alcohols and other compunds, which were not treated with MeOH, possess a residue of an alkane; it appears at ca. 0.8 ppm in the ^{1}H NMR spectra. Representative spectra are in the supplementary material.

IR spectra were obtained using the FT instrument Analect RFX-30 operating in ATR mode. A few drops of the compound of interest in CH_2Cl_2 were applied to the surface of a ZnSe ATR plate parallelogram (45°, Wilmad), and after the solvent evaporated, the spectrum was acquired (32 scans, 2-cm^{-1} resolution). Representative spectra are in the supplementary material.

Mass spectra were obtained at the Midwest Mass Spectrometry Center located on our campus. Representative spectra are in the supplementary material.

Elemental analyses were carried out by Dr. G. M. Dabkowski, Director—Microlytics, P.O. Box 199, S. Deerfield, MA 01373. The agreement between the calculated and found C/H analyses is improved when the alkane impurity (as "hexane equivalents" from integration of the 0.8 ppm and *tert*-Bu group peaks in the ^{1}H NMR spectra) and residual water are accounted for.

Steps AB and AC. *tert*-BuLi (2 equiv of a 1.7 M solution in pentane) was added to a 0.1–0.01 M suspension (or solution) of a bromo ether, ***N*-OMe-(OMe)$_n$-Br** (1 equiv), in ether at −78 °C. After the solution was stirred for 40 min at −78 °C, the temperature of the cooling bath was raised to −10 or 0°C for 2–5 min and, then, the ester (~0.5 equiv of methyl 3-bromo-2,4-dimethylbenzoate or methyl 4-*tert*-butylbenzoate) was added either neat or in ether. The reaction mixture was allowed to attain ambient temperature, and after 12–24 h, standard aqueous workup was performed. Removal of the solvents in vacuo gave a crude product, which appeared on a TLC silica plate below the reactant bromo ether. The product was separated by standard column chromatography at elevated pressure.

2-OH-(OMe)$_6$-Br: 1.50 g (80%), light yellow solid. FTIR: 3630 cm^{-1} (OH). Anal. Calcd for $C_{149}H_{179}O_7Br$: C, 82.78; H, 8.35. $C_{149}H_{179}O_7Br\cdot(H_2O)\cdot(C_6H_{14})$: C, 82.15; H, 8.67. Found: C, 82.53; H, 8.95. FABMS (3-NBA): Table I.

3-OH-(OMe)$_{14}$-Br: 1.24 g (70%), white solid. FTIR: 3400–3700 cm^{-1} br peak (OH). Anal. Calcd for $C_{309}H_{371}O_{15}Br$: C, 84.25; H, 8.49. $C_{309}H_{371}O_{15}Br\cdot(H_2O)_2\cdot(C_6H_{14})_2$: C, 83.57; H, 8.80. Found: C, 83.29; H, 8.87. FABMS (3-NBA): Table I.

4-OH-(OMe)$_{14}$: 0.649 g (90%), light yellow solid. FTIR: 3200–3700 cm^{-1} br peak (OH). Anal. Calcd for $C_{311}H_{376}O_{15}$: C, 85.79; H, 8.70. $C_{311}H_{376}O_{15}\cdot(C_6H_{14})_2$: C, 85.70; H, 9.00. Found: C, 85.60; H, 8.96. FABMS (3-NBA): Table I.

5-OH-(OMe)$_{30}$: 0.191 g (40%), yellow solid. FTIR: 3400–3700 cm^{-1} v weak (OH). FABMS (ONPOE): Table I.

Step D. The product from steps AB or AC, ***N*-OH-(OMe)$_n$-Br** or ***N*-OH-(OMe)$_n$**, 1 equiv, was added as a solid or a suspension (solution) in DMF to a suspension of NaH (10+ equiv) in DMF. The resultant 0.05–0.0025 M reaction mixture was stirred for 20 min. Subsequently, after brief cooling with an ice bath, MeI (~10 equiv) was added. After 5 h at ambient temperature, the reaction mixture solidified and the quenched reaction was quenched with MeOH, which was followed with aqueous workup. The product appeared on a TLC silica plate as a single spot slightly above that of the reactant. However, the resolution decreased for large molecular weights; all products, except for **5-OMe-(OMe)$_{30}$** and milligram-scale preparations, were separated by column chromatography at elevated pressure. IR spectra do not show any peaks in the 3200–3700 cm^{-1} range.[17]

2-OMe-(OMe)$_6$-Br: 2.80 g (75%), white solid. A sample for elemental analysis was treated with boiling MeOH. Anal. Calcd for $C_{150}H_{181}O_7Br$: C, 82.80; H, 8.38. Found: C, 83.00; H, 8.38. FABMS (3-NBA): Table I.

3-OMe-(OMe)$_{14}$-Br: 0.609 g (50%), white solid. Anal. Calcd for $C_{310}H_{373}O_{15}Br$: C, 84.25; H, 8.51. $C_{310}H_{373}O_{15}Br\cdot(H_2O)\cdot(C_6H_{14})_2$: C, 83.90; H, 8.81. Found: C, 83.92; H, 8.80. FABMS (3-NBA): Table I.

4-OMe-(OMe)$_{14}$. The single TLC spot fraction from chromatography (0.367 g) was treated with boiling MeOH (20 mL) to give 0.315 g (63%) of a white solid. Anal. Calcd for $C_{312}H_{378}O_{15}$: C, 85.78; H, 8.72. Found: C, 85.62; H, 8.48. FABMS (3-NBA, ONPOE): Table I.

4-O[^{13}C]Me-(OMe)$_{14}$ was prepared analogously to the nonlabeled product, except 99% ^{13}C MeI was used and no column chromatography was carried out; 15 mg (90+%). ^{13}C[^{1}H] NMR and ^{13}C DEPT 135° (C_6D_6, 295–350 K): δ 52.5 ($\Delta\delta_{1/2}$ 2). FABMS (ONPOE): Table I.

5-OMe-(OMe)$_{30}$, crude product, 0.147 g (80%), light yellow solid, possessed a single TLC spot overlapping the spot corresponding to **5-OH-(OMe)$_{30}$**. Anal. Calcd for $C_{632}H_{762}O_{31}$: C, 85.73; H, 8.67. $C_{632}H_{762}O_{31}\cdot(H_2O)_2\cdot(C_6H_{14})_2$: C, 85.34; H, 8.83. Found: C, 85.37; H, 9.11. FABMS (ONPOE): Table I.

Step E. 4-OMe-(OMe)$_{14}$ or **5-OMe-(OMe)$_{30}$** (12–20 mg) was stirred with an excess of lithium metal in THF (0.5 mL) for 7–10 days in a glovebox. Following the quenching with MeOH, standard aqueous workup and treatment with boiling MeOH (20 mL) provided the product.

4-H-(H)$_{14}$: 14 mg, light yellow solid. ^{1}H NMR (TCE/C_6D_6, 295 K): δ 7.2–5.8 (br), 5.5–4.6 (br), 2.4–0.7 (br); for these three regions, the integrations are in agreement with the 96:15:237 ratio. FABMS (ONPOE): Table I.

5-H-(H)$_{30}$: 16 mg, yellow solid. ^{1}H NMR (TCE/C_6D_6, 295 K): v br spectrum.

2-H-(H)$_6$-Br. Sodium borohydride pellets were added over a period of 1 h to a suspension of **2-OMe-(OMe)$_6$-Br** (96.3 mg) in MeOH (10 mL) and CF_3COOH (21 mL). After the solution was left overnight, ether (90 mL) was added and the mixture washed several times with 15% NaOH-(aq) and water. Drying over $MgSO_4$ and evaporation of the solvents gave yellow glass, which was purified by preparative TLC (hexane/ether, 20/1); light yellow solid, 54.6 mg (63%). ^{1}H NMR (TCE/C_6D_6, 370 K): δ 7.1–5.9 (46 H), 5.3, 5.3 (br, 4 H), 5.1, 5.1 (br, 3 H), 2.1–1.4 (42 H), 1.2–1.0 (72 H). FABMS (3-NBA): Table I.

Generation of Polyradicals and Magnetic Measurements. Solutions of the carbopolyanions in THF were obtained as in step E and, then, transferred to a special vessel and treated with a stoichiometric amount of I_2 at 180 K for 30–60 min on a vacuum line. (Crystals of I_2 were added under a stream of argon.) Polyradicals in THF were studied by SQUID. The special vessel, the procedures for the generation of polyradicals, and their SQUID measurements are already described for the lower homologues of the present polyradicals; please see: refs 6 and 11a.

Interpretation of Magnetic Measurements. The equation which relates magnetization M to the number of moles n of polyradical and the probability p for random occupation of each triarylmethyl site was derived as follows. For a polyradical with k sites and j defects, there will be $z_{kj} = k(k-1)...(k-j)/j!$ of defected polyradicals and $y_{kj} = z_{kj}(k-j)(j+1)/k$ of uncoupled spin systems with $S = {}^1/_2, ..., (k-j)/2$. For a given number of defects, $j < 5$, the number of spin systems *for each spin value* y_{kjS} is manually enumerated. Brillouin functions for each spin are multiplied by $nNg\mu_BS$, y_{kjS}, and $p^{(k-j)}(1-p)^j$ factors and added to obtain

$$M = n11160\sum\nolimits_S[\sum\nolimits_j y_{kjS}p^{(k-j)}(1-p)^j]\{(S+{}^1/_2)ctgh[(S+{}^1/_2)x] - ({}^1/_2)ctgh(x/2)\}$$

where $x = 1.34501[H/(T-\theta)]$ with H in T and T and θ in K. For a polyradical with 15 sites, $j > 4$ makes enumerations of the spin systems exceedingly laborious; consequently, for $j = 5$ and $j = 6$ defects, single Brillouin functions corresponding to $S = ({}^{15}/_2)/(j+1)$ are used. Similarly, for a polyradical with 31 sites, the $S = ({}^{31}/_2)/(j+1)$ Brillouin functions are used. This approximate procedure tends to overestimate the values for p.

The magnetic data were fit as follows. The MT vs T data, which were obtained at $H = 0.5$ T in the $T = 2$–80 K range, were fit to a derivative of the Curie–Weiss equation; when necessary, a factor correcting for uncompensated diamagnetism was also included, and subsequently, the remaining M vs H data were corrected for the diamagnetism. The M vs H data, which were obtained at $T = 2$, 5, and 10 K (in some instances, also 3 and 20 K) and in the $H = 0$–5.5-T range, were then treated according to the following sequence.

(1) Using θ from the Curie–Weiss equation and a guess, M_{sat}, the M/M_{sat} vs $H/(T-\theta)$ graphs were plotted; if needed, θ was adjusted until the curves coincided at all available temperatures.

(2) The M vs $H/(T-\theta)$ data at $T = 2$ K were fit to the above equation for M by simultaneous variation of n and p by standard numerical procedures.

(3) The p and n from the fit and $x > 20$ were substituted in the above equation to obtain M_{sat}, which was used for plotting both the experimental data and the fit as M/M_{sat} vs $H/(T-\theta)$.

The above procedure was repeated until a satisfactory fit was found.

Acknowledgment. We gratefully acknowledge the National Science Foundation, Chemistry Division, for the support of this research (CHE 9203918). Mass spectral determinations were performed by the Midwest Center for Mass Spectrometry with partial support by the National Science Foundation, Biology Division (DIR-9017262); we thank Dr. Ronald Cerny for obtaining the most challenging FAB spectra in the high m/e range. We thank Professor Sy-Hwang Liou for access to a SQUID magnetometer.

Supplementary Material Available: ^{1}H NMR spectra for compounds **2–5** and the solvent TCE/C_6D_6, IR spectra for polyethers ***N*-OMe-(OMe)$_n$-Br$_m$** (N = 2, 3, 4; n = 6, 14, 30; m = 0, 1) and the corresponding alcohols ***N*-OH-(OMe)$_n$Br$_m$** and mass spectra for **4-OMe-(OMe)$_{14}$**, **5-OMe-(OMe)$_{30}$**, the corresponding alcohols, and **4-O[^{13}C]Me-(OMe)$_{14}$** (31 pages). Ordering information is given on any current masthead page.